DC-AC Bridge Real-time Optimal Control based on a Reduced-Order Observer

Andres Escobar-Mejía, Eduardo Giraldo

***Abstract*—In this paper, a real-time optimal controller based on a reduced-order observer is proposed for an DC-AC Bridge. The state feedback optimal controller is designed considering a reduced-order state-space observer to estimate the magnetization current and the transformer's secondary current, which are highly difficult to sense due to their corresponding nature. The closed-loop controlled system is evaluated in simulation and over a Hardware-in-the-loop structure. The closed-loop response is evaluated in simulation and real-time by considering impulse and step references. The closed-loop response is also evaluated over additive noise conditions. In addition, the estimation error for the corresponding estimated variables is also considered.**

***Index Terms*—Embedded control, optimal control, real-time, AC-DC bridge.**

I. Introduction

SEVERAL approaches for real-time evaluation of controllers by using Hardware-In-the-Loop (HIL) structures or embedded controllers over scale prototypes have been proposed in the last years to close the gap between simulation and real-time implementation [1], [2], [3]. In [4], a hardware-in-the-loop (HIL) testing based on an FPGA is used to validate a complex system. The system includes two salient-pole synchronous machines, one permanent magnet synchronous machine, and encoders models, two full-wave six-pulse AC-DC diode bridge rectifiers, and one DC-DC buck converter. In [5] and [6] a linear and fractional-order PI controllers are evaluated over boost and buck converters by using HIL and embedded controllers structures.

The conventional DC-AC converter has been suggested in applications such as the front-end of a Dual Active Bridge (DAB), as described in [7], [8], which is the fundamental part of Solid State Transformer [9]. Also, the DC-AC converter has been studied in wireless power applications, as presented in [10] and [11]. In this case, the control of this converter determines the power flowing through the high-frequency transformer [12].

This work proposes a state feedback controller based on a reduced-order observer for an DC-AC bridge. The state feedback optimal controller is designed by considering a reduced-order state-space observer to estimate the magnetization current and the transformer's secondary current, which are highly difficult to sense due to their corresponding nature. The closed-loop controlled system is evaluated in simulation and over a Hardware-in-the-loop structure. The closed-loop response is evaluated in simulation and in real-time by considering impulse and step references. In addition, the estimation error for the corresponding estimated variables is also considered. This paper is organized as follows: In section II is presented the theoretical framework. In section III are presented the experimental setup, results, and discussions, and finally, in section IV are presented the final remarks and future works.

Manuscript received September 15, 2021; revised February 22, 2022.

Andres Escobar-Mejia is a full professor at the Department of Electrical Engineering, Universidad Tecnológica de Pereira, Pereira, Colombia. Research group in Power Electronics. E-mail: andreses1@utp.edu.co

Eduardo Giraldo is a full professor at the Department of Electrical Engineering, Universidad Tecnológica de Pereira, Pereira, Colombia. Research group in Automatic Control. E-mail: egiraldos@utp.edu.co

II. Theoretical framework

A. DC-AC Bridge Model

A complete description of an DC-AC converter is illustrated in Fig. 1.

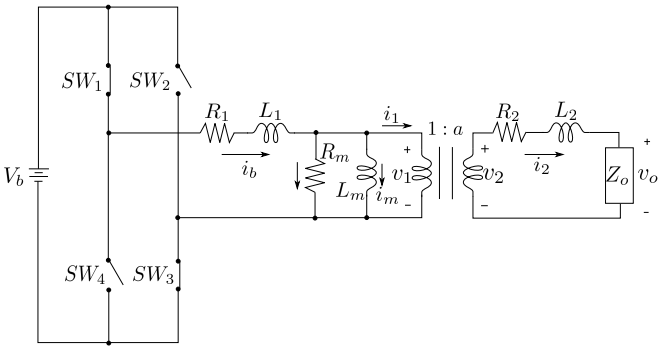

Fig. 1. DC-AC Bridge

It comprises a DC constant voltage source connected to a Full-Bridge connected to a high-frequency transformer. Series elements R_1, L_1 and R_2, L_2 represent the resistance and inductance of the primary and secondary windings. The resistance R_m models the core losses, and L_m is the magnetizing inductance. The load impedance is Z_o. The state-space model of the system in Fig. 1 is:

$$\begin{bmatrix} \frac{di_b}{dt} \\ \frac{di_m}{dt} \\ \frac{di_1}{dt} \end{bmatrix} = \begin{bmatrix} -\frac{R_1+R_m}{L_1} & \frac{R_m}{L_1} & \frac{R_m}{L_1} \\ \frac{R_m}{L_m} & -\frac{R_m}{L_m} & -\frac{R_m}{L_m} \\ \frac{R_m}{L'} & -\frac{R_m}{L'} & -\frac{R'+R_m}{L'} \end{bmatrix} \begin{bmatrix} i_b \\ i_m \\ i_1 \end{bmatrix} + \begin{bmatrix} \frac{V_b}{L_1} \\ 0 \\ 0 \end{bmatrix} u(t) \tag{1}$$

where the state variables are the Full-Bridge current output i_b, the magnetizing current i_m and the transformer primary current i_1. Furthermore,

$$\begin{aligned} R' &= \frac{R_2 + R_0}{a^2} \\ L' &= \frac{L_2 + L_0}{a^2} \end{aligned} \tag{2}$$

The measured output is the converter output current i_b, as follows:

$$\begin{bmatrix} y(t) \end{bmatrix} = \begin{bmatrix} 1 & 0 & 0 \end{bmatrix} \begin{bmatrix} i_b \\ i_m \\ i_1 \end{bmatrix} \tag{3}$$

It is worth noting that to design a state feedback controller, the magnetization current of the transformer i_m and the current on the primary on the transformer i_1 are estimated from the measured variable i_b.

B. Reduced-Order Observer

Since the converter output current i_b is measured directly from the system, only a reduced-order observer is required to estimate the magnetization current of the transformer i_m, and the current on the primary on the transformer i_1, as described in (1). In [13], a reduced-order observer is presented by defining

$\mathbf{x}_1$: state vector of measurements.
$\mathbf{x}_2$: state vector to be estimated.

The state-space model of (1) can be decomposed as follows:

$$\begin{bmatrix} \dot{\mathbf{x}}_1 \\ \dot{\mathbf{x}}_2 \end{bmatrix} = \begin{bmatrix} \mathbf{A}_{11} & \mathbf{A}_{12} \\ \mathbf{A}_{21} & \mathbf{A}_{22} \end{bmatrix} \begin{bmatrix} \mathbf{x}_1 \\ \mathbf{x}_2 \end{bmatrix} + \begin{bmatrix} \mathbf{B}_1 \\ \mathbf{B}_2 \end{bmatrix} \mathbf{u} \tag{4}$$

where

$$\begin{aligned} \mathbf{A}_{11} &= \begin{bmatrix} -\frac{R_1+R_m}{L_1} \end{bmatrix} \\ \mathbf{A}_{12} &= \begin{bmatrix} \frac{R_m}{L_1} & \frac{R_m}{L_1} \end{bmatrix} \\ \mathbf{A}_{21} &= \begin{bmatrix} \frac{R_m}{L_m} \\ \frac{R_m}{L'} \end{bmatrix} \\ \mathbf{A}_{22} &= \begin{bmatrix} -\frac{R_m}{L_m} & -\frac{R_m}{L_m} \\ -\frac{R_m}{L'} & -\frac{R'+R_m}{L'} \end{bmatrix} \end{aligned} \tag{5}$$

and

$$\begin{aligned} \mathbf{B}_1 &= \begin{bmatrix} \frac{V_b}{L_1} \end{bmatrix} \\ \mathbf{B}_2 &= \begin{bmatrix} 0 \\ 0 \end{bmatrix} \end{aligned} \tag{6}$$

In addition, the measurement equation of (3) can be divided as follows

$$\mathbf{y} = \begin{bmatrix} \mathbf{C}_1 & \mathbf{C}_2 \end{bmatrix} \begin{bmatrix} \mathbf{x}_1 \\ \mathbf{x}_2 \end{bmatrix} \tag{7}$$

being

$$\begin{aligned} \mathbf{C}_1 &= \begin{bmatrix} 1 \end{bmatrix} \\ \mathbf{C}_2 &= \begin{bmatrix} 0 & 0 \end{bmatrix} \end{aligned} \tag{8}$$

Therefore $\mathbf{x}_1$ can be obtained as:

$$\mathbf{x}_1 = \mathbf{y} \tag{9}$$

From (4), the equations for $\mathbf{x}_1$ y $\mathbf{x}_2$ can be obtained as follows:

$$\begin{aligned} \dot{\mathbf{x}}_1 &= \mathbf{A}_{11}\mathbf{x}_1 + \mathbf{A}_{12}\mathbf{x}_2 + \mathbf{B}_1\mathbf{u} \\ \dot{\mathbf{x}}_2 &= \mathbf{A}_{21}\mathbf{x}_1 + \mathbf{A}_{22}\mathbf{x}_2 + \mathbf{B}_2\mathbf{u} \end{aligned} \tag{10}$$

by using (10), the following output equation can be obtained

$$\dot{\mathbf{x}}_1 - \mathbf{A}_{11}\mathbf{x}_1 - \mathbf{B}_1\mathbf{u} = \mathbf{A}_{12}\mathbf{x}_2 \tag{11}$$

where $\dot{\mathbf{x}}_1 - \mathbf{A}_{11}\mathbf{x}_1 - \mathbf{B}_1\mathbf{u}$ are known. Equation (10) can be rewritten as follows:

$$\dot{\mathbf{x}}_2 = \mathbf{A}_{22}\mathbf{x}_2 + \mathbf{A}_{21}\mathbf{x}_1 + \mathbf{B}_2\mathbf{u} \tag{12}$$

where $\mathbf{A}_{21}\mathbf{x}_1 + \mathbf{B}_2\mathbf{u}$ are known. Equation (10) describes the dynamical model of the state variables to be estimated. For these variables, the following observer can be defined:

$$\dot{\tilde{\mathbf{x}}}_2 = \mathbf{A}_{22}\tilde{\mathbf{x}}_2 + \mathbf{A}_{21}\mathbf{x}_1 + \mathbf{B}_2\mathbf{u} + \mathbf{L}\left(\mathbf{y}' - \mathbf{C}'\tilde{\mathbf{x}}_2\right) \tag{13}$$

where $\mathbf{y}'$ are the known variables of (11) given by:

$$\mathbf{y}' = \dot{\mathbf{x}}_1 - \mathbf{A}_{11}\mathbf{x}_1 - \mathbf{B}_1\mathbf{u} = \mathbf{A}_{12}\mathbf{x}_2 \tag{14}$$

with $\mathbf{C}' = \mathbf{A}_{12}$. As a result, the reduced-order equation is obtained as follows:

$$\begin{aligned} \dot{\tilde{\mathbf{x}}}_2 =& \mathbf{A}_{22}\tilde{\mathbf{x}}_2 + \mathbf{A}_{21}\mathbf{x}_1 + \mathbf{B}_2\mathbf{u} \\ &+ \mathbf{L}\left(\dot{\mathbf{x}}_1 - \mathbf{A}_{11}\mathbf{x}_1 - \mathbf{B}_1\mathbf{u} - \mathbf{A}_{12}\tilde{\mathbf{x}}_2\right) \end{aligned} \tag{15}$$

By rewritten (15), the following equation is obtained

$$\begin{aligned} \dot{\tilde{\mathbf{x}}}_2 =& \left(\mathbf{A}_{22} - \mathbf{L}\mathbf{A}_{12}\right)\tilde{\mathbf{x}}_2 + \mathbf{A}_{21}\mathbf{x}_1 + \mathbf{B}_2\mathbf{u} \\ &+ \mathbf{L}\left(\dot{\mathbf{x}}_1 - \mathbf{A}_{11}\mathbf{x}_1 - \mathbf{B}_1\mathbf{u}\right) \end{aligned} \tag{16}$$

being $\mathbf{A}_{21}\mathbf{x}_1 + \mathbf{B}_2\mathbf{u} + \mathbf{L}\left(\dot{\mathbf{x}}_1 - \mathbf{A}_{11}\mathbf{x}_1 - \mathbf{B}_1\mathbf{u}\right)$ known. However, in (16) it is necessary to obtain the term $\dot{\mathbf{x}}_1$. To do this, equation (16) is rewritten as follows:

$$\begin{aligned} \dot{\tilde{\mathbf{x}}}_2 - \mathbf{L}\dot{\mathbf{x}}_1 =& \left(\mathbf{A}_{22} - \mathbf{L}\mathbf{A}_{12}\right)\tilde{\mathbf{x}}_2 + \left(\mathbf{A}_{21} - \mathbf{L}\mathbf{A}_{11}\right)\mathbf{x}_1 \\ &+ \left(\mathbf{B}_2 - \mathbf{L}\mathbf{B}_1\right)\mathbf{u} \end{aligned} \tag{17}$$

and by adding the term $\left(\mathbf{A}_{22} - \mathbf{L}\mathbf{A}_{12}\right)\mathbf{L}\mathbf{x}_1$ to (17), the following equation can be obtained:

$$\begin{aligned} \dot{\tilde{\mathbf{x}}}_2 - \mathbf{L}\dot{\mathbf{x}}_1 =& \left(\mathbf{A}_{22} - \mathbf{L}\mathbf{A}_{12}\right)\left(\tilde{\mathbf{x}}_2 - \mathbf{L}\mathbf{x}_1\right) \\ &+ \left[\left(\mathbf{A}_{21} - \mathbf{L}\mathbf{A}_{11}\right) + \left(\mathbf{A}_{22} - \mathbf{L}\mathbf{A}_{12}\right)\mathbf{L}\right]\mathbf{x}_1 \\ &+ \left(\mathbf{B}_2 - \mathbf{L}\mathbf{B}_1\right)\mathbf{u} \end{aligned} \tag{18}$$

being $\tilde{\eta} = \left(\tilde{\mathbf{x}}_2 - \mathbf{L}\mathbf{x}_1\right)$, equation (18) can be rewritten as follows:

$$\begin{aligned} \dot{\tilde{\eta}} =& \left(\mathbf{A}_{22} - \mathbf{L}\mathbf{A}_{12}\right)\tilde{\eta} \\ &+ \left[\left(\mathbf{A}_{21} - \mathbf{L}\mathbf{A}_{11}\right) + \left(\mathbf{A}_{22} - \mathbf{L}\mathbf{A}_{12}\right)\mathbf{L}\right]\mathbf{x}_1 \\ &+ \left(\mathbf{B}_2 - \mathbf{L}\mathbf{B}_1\right)\mathbf{u} \end{aligned} \tag{19}$$

It is worth noting that (19) describes the dynamics of the reduced-order observer. In Fig. 2 is shown the reduced-order observer by including a state feedback controller.

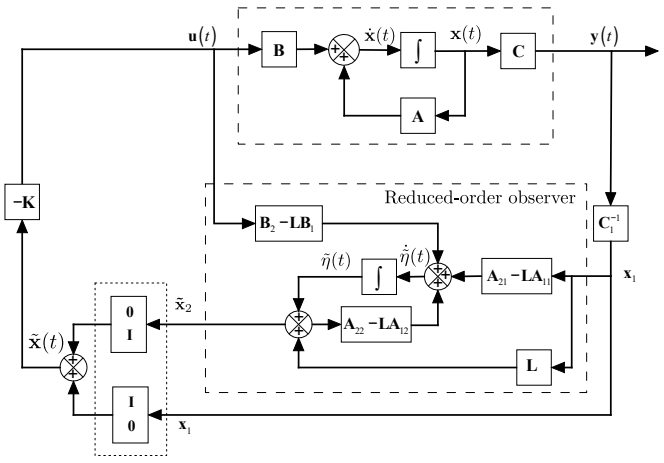

Fig. 2. Reduced-order observer

It can be seen, that the complete state vector $\tilde{\mathbf{x}}$ can be obtained as follows:

$$\tilde{\mathbf{x}} = \begin{bmatrix} \mathbf{I} \\ \mathbf{0} \end{bmatrix} \mathbf{x}_1 + \begin{bmatrix} \mathbf{0} \\ \mathbf{I} \end{bmatrix} \tilde{\mathbf{x}}_2 \tag{20}$$

where $\mathbf{L}$ is computed from the dual system $\mathbf{A}_{22}^T - \mathbf{A}_{12}^T \mathbf{L}^T$ as in the full order observer.

It is worth mentioning that the rank for observability matrix $\mathcal{O}$ of (1) for the full-order observer is 2, as follows:

$$\mathcal{O} = \begin{bmatrix} C \\ CA \\ CA^2 \end{bmatrix} \tag{21}$$

where $rank(\mathcal{O}) = 2$ and therefore a full-order observer can not be designed since the rank must be 3. However, for the reduced-order observer, the computed rank of the observability matrix $\mathcal{O}_{ro}$ is also 2, as follows:

$$\mathcal{O}_{ro} = \begin{bmatrix} A_{12} \\ A_{12}A_{22} \end{bmatrix} \tag{22}$$

where $rank(\mathcal{O}) = 2$ and therefore, a reduced-order observer can be designed.

C. HIL Structure

A HIL structure of the proposed system is used for evaluation of the system over a real-time embedded controller. To this end, a block diagram as presented in Fig. 3 is used, where the state space model of (1) is used in discrete time.

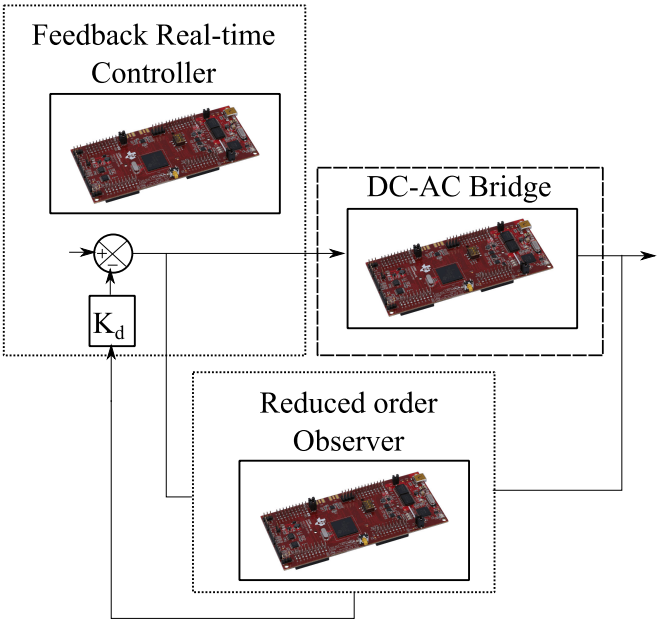

Fig. 3. HIL structure for validation

The reduced-order observer of (19) is also computed in discrete-time as a differences equation.

III. Results

The performance of the proposed approach is evaluated over a DC-AC Bridge by considering the following parameters: $R_1 = 0.02\Omega$, $R_m = 200\Omega$, $L_1 = 10e-6$H, $L_m = 0.16e-6$H, $V_b = 24$V, $R_2 = 0.1\Omega$, $R_0 = 23\Omega$, $a = 5$, $R_p = (R_2 + R_0)/a^2$, $L_2 = 50e-6$H, $L_0 = 18e-3$H, $L_p = (L_2 + L_0)/a^2$, $f = 60$kHz. The system is evaluated under simulation for continuum and discrete time. Two cases are analyzed, the impulse response and the step response, where the output of the system, the estimation error, and state vector transient performance are considered.

The feedback gain of the state feedback control is computed by using a Linear Quadratic Regulator (LQR), as follows $K = \begin{bmatrix} 1.39009 & 0.02329 & -0.68343 \end{bmatrix}$.

The closed-loop response for an impulse reference tracking is presented in Fig. 4.

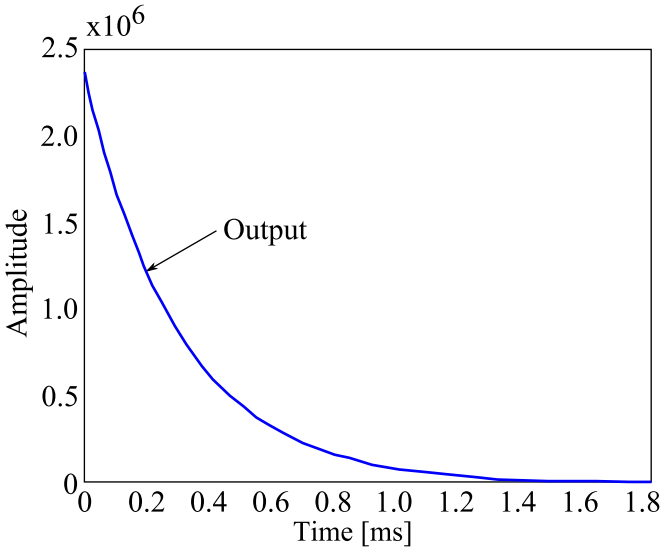

Fig. 4. Impulse response for reference tracking of the closed loop system

The closed-loop state space response for an impulse reference tracking is presented in Fig. 5.

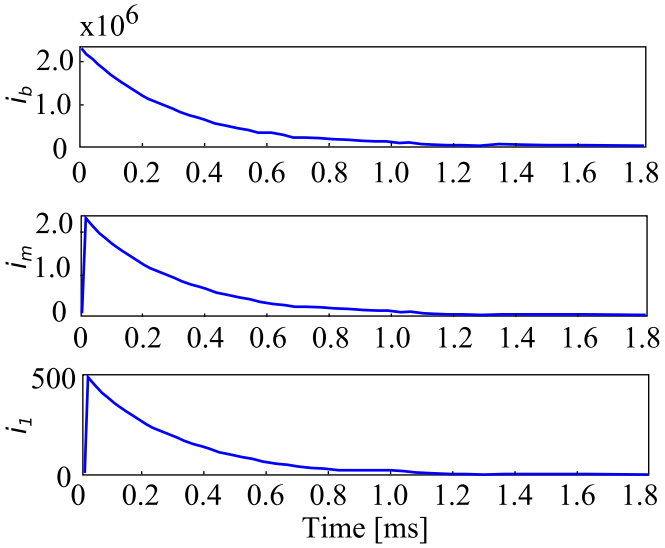

Fig. 5. Impulse response of the state-space vector of the closed loop system

The reduced-order observer gain L is also computed by using a LQR, obtaining $L = \begin{bmatrix} 0.008 & 0.008 \end{bmatrix}^T$.

The closed-loop estimation error response for an impulse reference tracking is presented in Fig. 6.

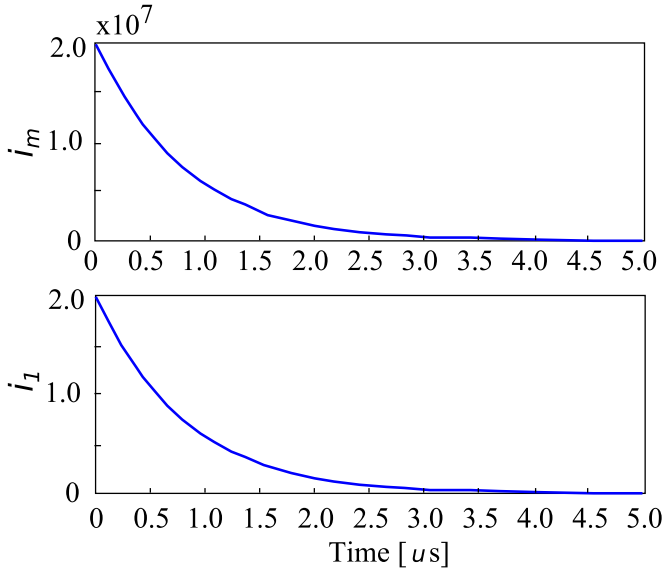

Fig. 6. Estimation error of the reduced-order state-space vector of the closed-loop system

It can be seen that in Fig. 6 the estimation errors computed from i_m and i_1 and their corresponding estimated values tend to zero around 4μs. It is worth noting that in Fig. 9 the signal reach their reference value around 1.2ns.

The closed-loop control signal for an impulse reference is presented in Fig. 7.

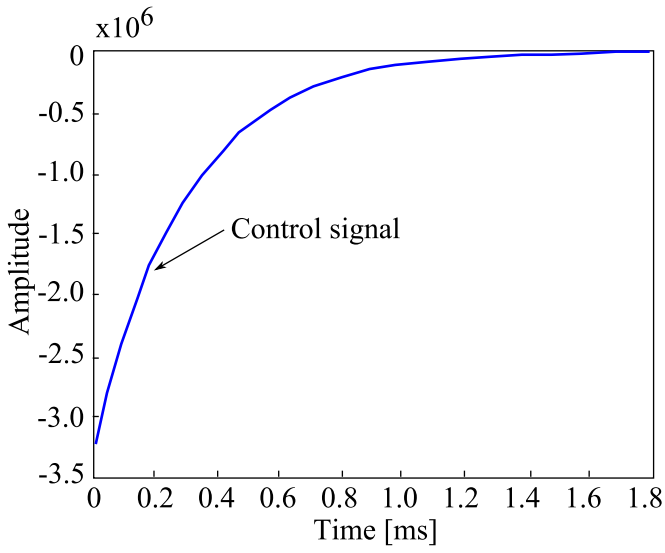

Fig. 7. Control signal for Impulse reference of the closed-loop system

The closed-loop response for a step reference tracking is presented in Fig. 8.

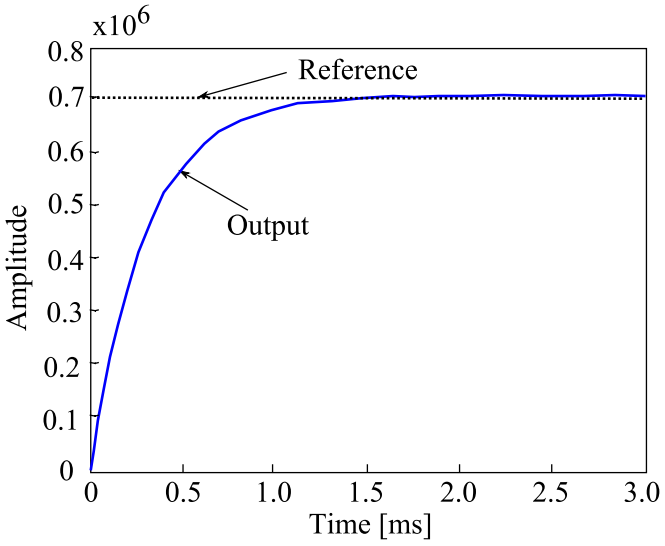

Fig. 8. Step reference tracking of the closed-loop system

The closed loop state space response for a step reference tracking is presented in Fig. 9.

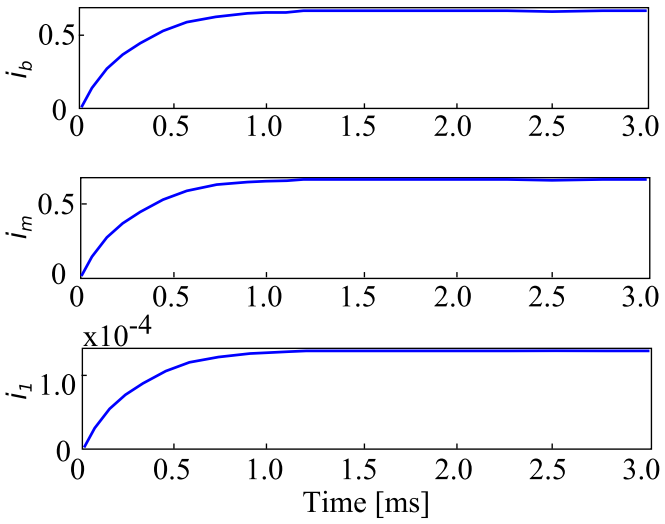

Fig. 9. Step response of the state-space vector of the closed-loop system

The discrete state-space model is obtained by using a sample time of 0.1 microseconds.

The discrete feedback gain of the state feedback control is computed by using a discrete Linear Quadratic Regulator (dLQR), obtaining the $K_d = \begin{bmatrix} 1.178127 & 0.018978 & -0.57962 \end{bmatrix}$.

The closed-loop response in discrete time for an impulse reference tracking is presented in Fig. 10.

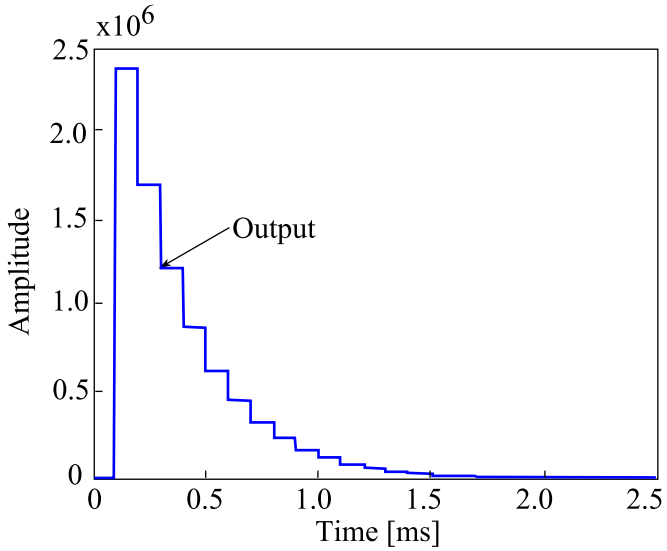

Fig. 10. Impulse reference tracking of the closed-loop system in discrete time

The closed-loop state space response in discrete-time for an impulse reference tracking is presented in Fig. 11.

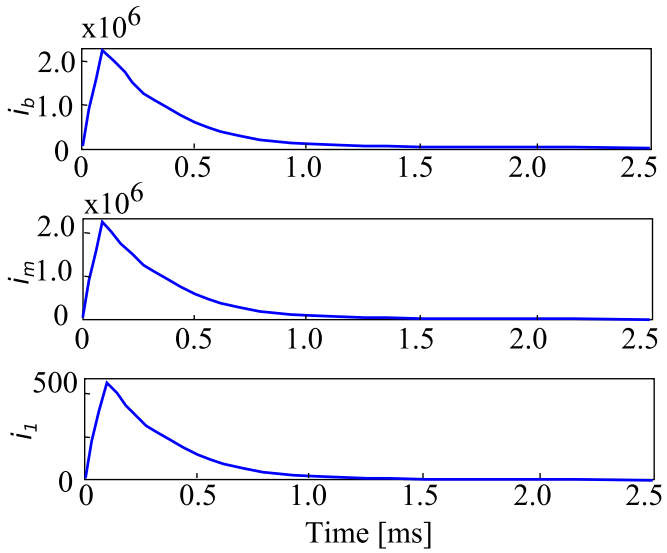

Fig. 11. Impulse response of the state-space vector of the closed-loop system in discrete time

The closed-loop control signal for an impulse reference is presented in Fig. 12.

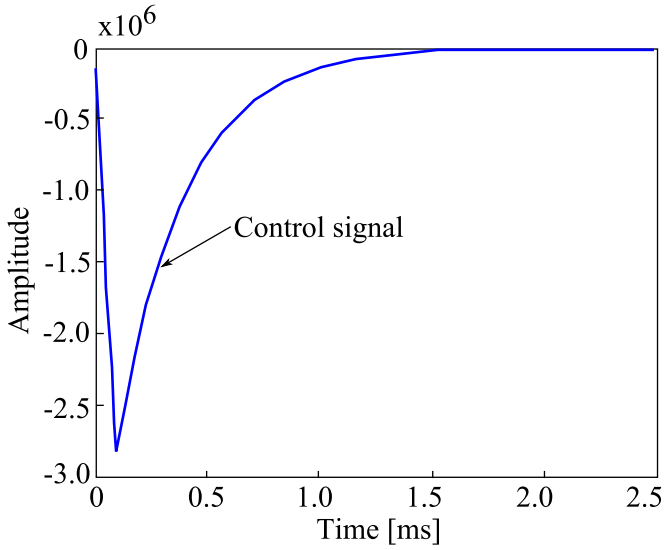

Fig. 12. Control signal for Impulse reference of the closed-loop system in discrete time

An additional analysis is performed under noise conditions, by assuming a 10% additive noise at the output. As a result, the impulse response is presented in Fig. 13.

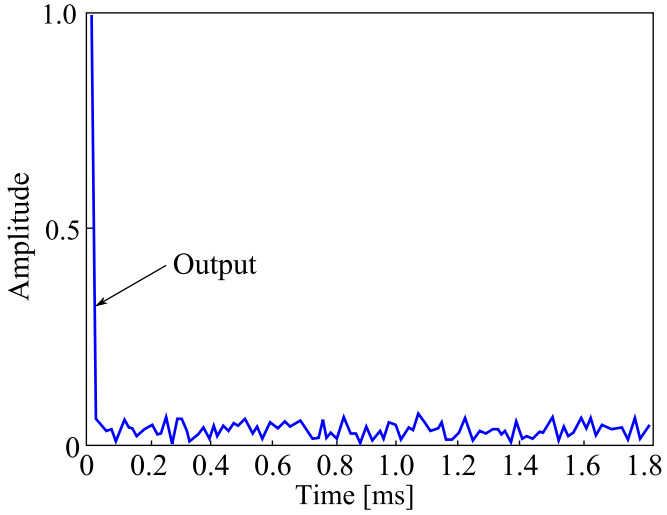

Fig. 13. Impulse reference tracking of the closed-loop system under 10% additive noise

It can be seen that the closed-loop system adequately follows the zero reference even under noise conditions.

In addition an analysis under noise conditions is also performed for a step reference. To this end, the step response is presented in Fig. 14.

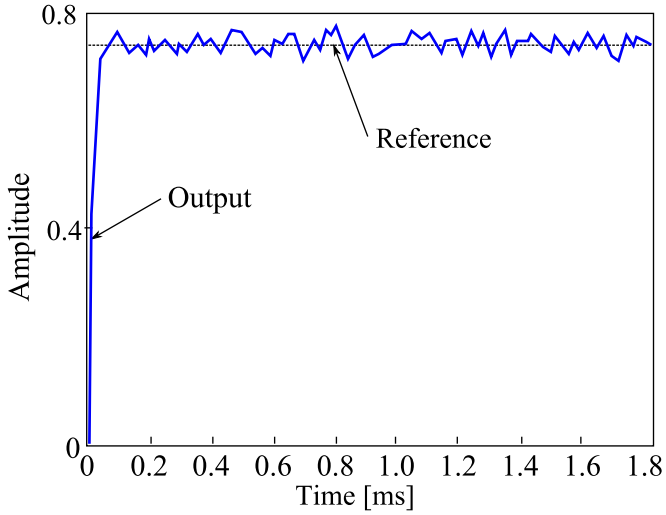

Fig. 14. Step reference tracking of the closed-loop system under 10% additive noise

It can be seen that the closed-loop system adequately follow the step reference even under noise conditions.

In order to evaluate the robustness of the proposed approach, and also under noise conditions, an analysis under step additive disturbances at the output is also performed for a step reference, where the disturbance is applied at time $t = 1$ second. To this end, the tracking response is presented in Fig. 15.

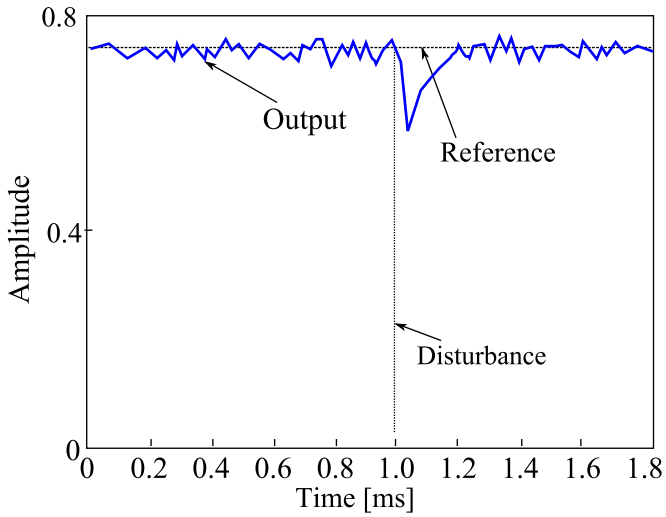

Fig. 15. Step reference tracking of the closed-loop system under 10% additive noise and additive disturbance at the output at $t = 1$ second

It can be seen that the closed-loop system adequately follow the step reference even under additive disturbances and noise conditions.

IV. Conclusions

In this work, a state feedback controller is proposed based on a reduced-order observer for a DC-AC Bridge. The state feedback optimal controller is designed by considering a reduced-order state-space observer for estimation of the magnetization current and the transformer's secondary current. As a result, the estimation of two variables that are highly difficult to sense due to their corresponding nature is achieved. The system is validated even under noise conditions, where the proposed approach effectively tracks impulse and step references even under step additive disturbances. In addition, the validation of the proposed optimal approach over a HIL environment allows evaluating the system performance in real-time. This evaluation can be made due to the real-time measurements resulting from an embedded controller.

References

[1] E. Giraldo, "Real-time control of a magnetic levitation system for time-varying reference tracking," *IAENG International Journal of Applied Mathematics*, vol. 51, no. 3, pp. 792–798, 2021.

[2] M. Bueno-Lopez and E. Giraldo, "Real-time decentralized control of a hardware-in-the-loop microgrid," *IAENG International Journal of Computer Science*, vol. 48, no. 3, pp. 653–662, 2021.

[3] B. Lu, X. Wu, H. Figueroa, and A. Monti, "A low-cost real-time hardware-in-the-loop testing approach of power electronics controls," *IEEE Transactions on Industrial Electronics*, vol. 54, no. 2, pp. 919–931, 2007.

[4] B. Jandaghi, L.-A. Grégoire, J. V. Nava, S. Cense, and J. Bélanger, "Fpga-based real-time simulation of a three-stage energy conversion system in electric aircrafts," in *2020 IEEE Power Energy Society General Meeting (PESGM)*, 2020, pp. 1–5.

[5] E. Giraldo, "Real-time modified pid controller over a dc-dc boost converter," *IAENG International Journal of Applied Mathematics*, vol. 51, no. 3, pp. 892–898, 2021.

[6] M. Bueno-Lopez and E. Giraldo, "Real-time fractional order pi for embedded control of a synchronous buck converter," *Engineering Letters*, vol. 29, no. 3, pp. 1212–1219, 2021.

[7] A. Marin-Hurtado, E. Piedrahita-Echavarria, and A. Escobar-Mejia, "Modeling and control of two dc-dc convertes used in a resonant dual active bridge," in *2018 IEEE ANDESCON*, 2018, pp. 1–5.

[8] D. Gonzalez-Agudelo, A. Escobar-Mejía, and H. Ramirez-Murrillo, "Dynamic model of a dual active bridge suitable for solid state transformers," in *2016 13th International Conference on Power Electronics (CIEP)*, 2016, pp. 350–355.

[9] L. A. Garcia-Rodriguez, J. C. Balda, A. Mallela, and A. Escobar-Mejía, "A new sst topology comprising boost three-level ac/dc converters for applications in electric power distribution systems," in *2015 IEEE Energy Conversion Congress and Exposition (ECCE)*, 2015, pp. 6051–6058.

[10] S. Samanta and A. K. Rathore, "A new current-fed clc transmitter and lc receiver topology for inductive wireless power transfer application: Analysis, design, and experimental results," *IEEE Transactions on Transportation Electrification*, vol. 1, no. 4, pp. 357–368, 2015.

[11] H. Ota, J. Liu, Y. Miura, Y. Yanagisawa, A. Wada, S. Sakabe, H. Bevrani, and T. Ise, "Multiphase direct ac wireless power transfer system: Comparative proposals using frequency and amplitude modulations," *IEEE Journal of Emerging and Selected Topics in Industrial Electronics*, vol. 2, no. 2, pp. 101–112, 2021.

[12] A. Nahavandi, M. Roostaee, and M. R. Azizi, "Single stage dc-ac boost converter," in *2016 7th Power Electronics and Drive Systems Technologies Conference (PEDSTC)*, 2016, pp. 362–366.

[13] E. Giraldo, *Multivariable Control*. Germany: Scholar's Press, 2016.